NUCLEAR THEORY, Vol. 39 (2022)
eds. M. Gaidarov, N. Minkov, Heron Press, Sofia

Influence of Momentum Dependent Interactions on the Energy of Onset of Vaporization

Navjot K. Dhillon, **Sakshi Gautam**, **Rajeev K. Puri**

[1]Department of Physics, Panjab University, 160014, Chandigarh

Abstract. We have studied the onset of vaporization in ^{16}O + ^{80}Br and ^{16}O + ^{107}Ag collisions using Quantum Molecular Dynamics (QMD) calculations supplemented with Simulated Annealing Clusterization Algorithm (SACA) for fragment formation. The calculations are compared with available experimental measurements and our findings reveal a reasonably good agreement with the data. Further, the collisions of ^{40}Ca + ^{40}Ca and ^{197}Au + ^{197}Au are studied for understanding the role of total colliding mass and influence of momentum dependent interactions on the onset of vaporization. In addition to average charge, gas/liquid content of fragmenting system is examined to infer about the onset of vaporization. This study is still in progress to further search new observables which could probe the onset of vaporization in a sophisticated manner.

1 Introduction

Phase transitions are interesting phenomenon which occurs in heavy-ion reactions. The excited system formed during heavy ion collisions can decay via various channels. At low excitation energies, fusion or deep inelastic reaction occurs followed by evaporation. At intermediate energies, excited nuclear system will breakup into many fragments, such phenomenon is known as nuclear multifragmentation. At high energies system breaks up into light particles forming the gas phase. This process is termed as nuclear vaporization. The phenomenon of multifragmentation is very well established but nuclear vaporization is still under investigation. Many experimental observables have been used to study the nuclear liquid-gas phase transition. Some of these are rise and fall of multiplicity of intermediate mass fragments, nuclear caloric curve, isospin fractionation, moments of charge distribution, etc.

Jakobson *et al.* [1] studied the ^{16}O + ^{80}Br and ^{16}O + ^{107}Ag reactions at energies ranging from 10 MeV/nucleon to 220 MeV/nucleon. It was noted that at high energies above 50 MeV/nucleon, medium sized fragments are emitted at central collisions. The charge distribution gets narrow down with increase in energy and for the most central collisions, it shows a smooth transition from fusion to multifragmentation. The average charge as a function of energy is studied with and without the largest fragment included. If the heaviest fragment

is excluded then it is observed that the average charge is nearly constant indicating that the increased amount of excitation energy is mainly used to breakup the heaviest fragment asymmetrically. But clear signal of critical behaviour is not observed. Souza *et al.* [2] studied the ^{16}O + ^{80}Br reactions at bombarding energies ranging from 50 to 200 MeV/nucleon. The calculations are performed with Quantum Molecular Dynamics (QMD) model supported with restructured aggregation model. The evolution of average charge of fragments (with and without largest fragment) as a function of bombarding energies is studied. As the bombarding energy increases, the system breaks into more and more fragments untill a situation is reached when system disassembles completely into free nucleons. This is approved by system average charge approaching unity at 200 MeV/nucleon. The average charge excluding the largest fragment remains constant with value unity for energies above 50 MeV/nucleon. Thus, main de-excitation mechanism of system is emission of light fragments at high energies depicting the phenomenon of vaporization. This feature is further supported by Souza *et al.* by studying the multiplicity of all charged particles and IMF as a function of bombarding energy and compairing the results it is inferred that above 150 MeV/nucleon system disassembly gives less IMF and more light particles.

In this work we aim to study the energy of onset of vaporization. We have studied the collisions of ^{16}O + ^{80}Br and ^{16}O + ^{107}Ag at various energies ranging from 10 to 220 MeV/nucleon as emulsion data is available for these collisions. We have studied the collisions of ^{40}Ca + ^{40}Ca and ^{197}Au + ^{197}Au. At first we have looked into the average charge of the fragments and it is inferred that when average charge approaches unity then nuclear vaporization has started. This is further supported by studying the free nucleons and bound particles content of the system. The influence of momentum dependent interactions on the energy of onset of vaporization is primarily studied.

2 Model

Our present analysis is carried out using Quantum Molecular Dynamics (QMD) [3, 4] model. It is a many-body approach which gives us detailed information about the phase-space of nucleons on an event-by-event basis. The wave function of each nucleon is represented by a Gaussian wave packet in coordinate and momentum space and is of the form:

$$\psi_i(\mathbf{r}, \mathbf{r}_i(t), \mathbf{p}_i(t)) = \frac{1}{(2\pi L)^{3/4}} \exp\left[\frac{i}{\hbar}\mathbf{p}_i(t)\cdot\mathbf{r} - \frac{(\mathbf{r}-\mathbf{r}_i(t))^2}{4L}\right]. \quad (1)$$

The Gaussian width 'L' is centered around the mean position $\mathbf{r}_i$(t) and mean momentum $\mathbf{p}_i$(t), and is kept constant for all the nucleons. During the reactions, the centroids of each wave packet follow the Hamilton's equations of motion:

$$\dot{\mathbf{r}}_i = \frac{\partial\langle H\rangle}{\partial\mathbf{p}_i}; \qquad \dot{\mathbf{p}}_i = -\frac{\partial\langle H\rangle}{\partial\mathbf{r}_i}. \quad (2)$$

Here, 'H' stands for the Hamiltonian of the system, consisting of kinetic and potential parts and is represented by:

$$\langle H \rangle = \langle T \rangle + \langle V \rangle = \sum_i \frac{\mathbf{p}_i^2}{2m_i} + V^{\text{Sky}} + V^{\text{Yuk}} + V^{\text{Coul}}. \quad (3)$$

The terms V^{Sky}, V^{Yuk} and V^{Coul} are the local (two and three-body) Skyrme, Yukawa and Coulomb potentials, respectively. We follow the trajectory of each nucleon during the evolution and thus store the phase space of all nucleons. The phase space is then subjected to various cluster identification algorithms. The clusterization algorithm used here is Simulated Annealing Clusterization Algorithm (SACA) [5]. Based on the idea of energy minimization, Puri *et al.* designed a unique clusterization technique "Simulated Annealing Clusterization Algorithm (SACA)" [5]. This algorithm is able to recognize the correlations among nucleons bound in fragments much ahead of their formal separation in coordinate space. SACA enables one to understand the reaction dynamics at the violent stages of a reaction. Here, Monte-Carlo simulated annealing technique is evoked to search for the most bound configuration consisting of the fragments of different sizes and free nucleons. This algorithm constructs almost all possible fragment configurations using metropolis procedure [6] coupled with "simulated annealing" technique [7]. This algorithm is a sequence of metropolis steps with a control parameter ϑ interpreted as "temperature".

Further, it may happen that at intermediate times of a reaction too many clusters are recognized, which will break apart at later times. To avoid this and to fasten the procedure the pre-clusters formed at the intermediate stages are subjected to following binding energy condition:

$$\zeta = \sum_{i=1}^{A_f} \left[\sqrt{(\mathbf{p}_i - \mathbf{p}_{A_f}^{\text{cm}})^2 + m_i^2} - m_i + \frac{1}{2} \sum_{j \neq i}^{A_f} V_{ij}(\mathbf{r}_i, \mathbf{r}_j) \right] < E_{\text{bind}} \times A_f, \quad (4)$$

with $E_{\text{bind}} = -4.0$ MeV, if $A_f \geq 3$ and $E_{\text{bind}} = 0$ MeV, otherwise. This constant binding energy cut was changed to microscopic binding energy cut, where binding energy is calculated using the binding energy formula. But the effect on final fragment configuration has been seen to be insignificant. This condition assists to realize the fragments early, despite the fact that if once loosely bound fragments are formed, it consumes longer time to search for the true configuration. The steps for SACA algorithm reads as:

1. One begins from any random configuration 'ψ'' having energy $\zeta_{\psi'}$. From which a new fragment configuration 'ϕ'' with energy $\zeta_{\phi'}$ is generated using Monte-Carlo procedure. This is done by shifting one or few nucleons from one fragment to other fragment.

2. The energy difference between the old and new fragment configuration is calculated i.e., $\Delta\zeta = \zeta_{\phi'} - \zeta_{\psi'}$.

3. If energy difference between two configurations ($\Delta\zeta$) is negative, the new configuration is always accepted. On the other hand, if $\Delta\zeta$ is positive, the new configuration is still accepted with a probability $\exp(-\Delta\zeta/\vartheta)$ to avoid any local minima.

This procedure is known as Metropolis algorithm. The control parameter is then decreased in small steps. This algorithm will eventually yield the most bound configuration (MBC). Since this combination of a Metropolis algorithm with decreasing control parameter is known as simulated annealing, this approach was dubbed as Simulated Annealing Clusterization Algorithm (SACA).

3 Results and Discussion

To study the phenomenon of vaporization, the phase space of nucleons is generated using the Quantum Molecular Dynamical (QMD) model and fragment formation is done using Simualated Annealing Clusterization Algorithm (SACA). At first, we have compared the model calculations with the available experimental data for the $^{16}O + {}^{80}Br$ and $^{16}O + {}^{107}Ag$ reactions. We have used the soft equation of state along with energy dependent cross-section. In Figure 1 we have shown the dependence of average charge on the incident energy for the reactions of $^{16}O + {}^{80}Br$ (top panels) and $^{16}O + {}^{107}Ag$ (bottom panels). The av-

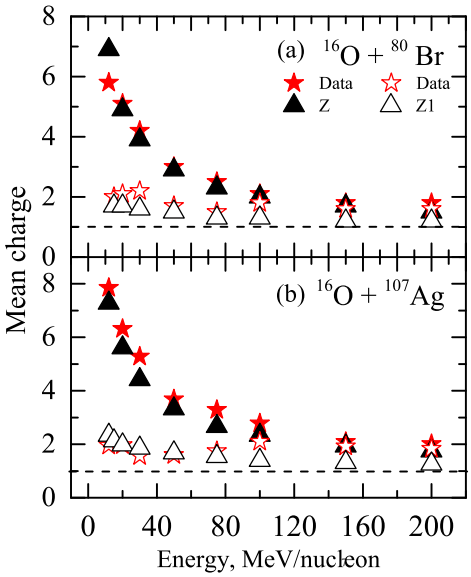

Figure 1. The energy dependence of average charge of fragments as a function of bombarding energy for the reactions of (a) $^{16}O + {}^{80}Br$ (top panels) and (b) $^{16}O + {}^{107}Ag$ (bottom panels).

erage charge is calculated with ($\langle Z \rangle$) (closed symbols) and without ($\langle Z_1 \rangle$) (open symbols) largest fragment. The stars correspond to the experimental data and triangles represent the model calculations. With increase in excitation energy, average charge decreases, approaches unity, indicating the onset of vaporization.

Next, we have studied the ^{40}Ca + ^{40}Ca and ^{197}Au + ^{197}Au reactions at central colliding geometry ($\hat{b}$ = 0.0-0.25) to look for the influence of momentum dependent interactions on the energy of onset of vaporization. Momentum dependence of the mean field plays a very important role in deciding the dynamics of the heavy-ion collisions [8–11]. During the early stages of the reaction when projectile and target are at distance from each other, then relative momentum of nucleons is very small and momentum dependent interactions are not dominant. But as the reaction proceeds, relative momentum between the projectile and target increases, resulting in the repulsions in the overlap region. In Figure 2, we have shown the average charge of fragments with (closed symbols, left panels) and without (open symbols, right panels) the largest fragment. Here triangles represent the results without momentum dependent interactions whereas circles represents the results with momentum dependent interactions. We observe that average charge do not show much effect of momentum dependent interactions and onset of vaporization is observed to begin between 200–300 MeV/nucleon.

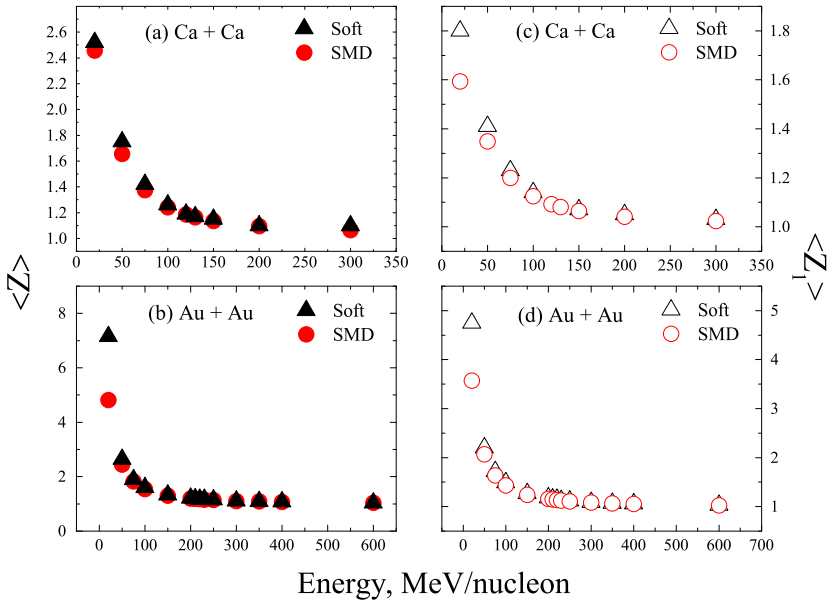

Figure 2. The average charge of fragments for the collisions of (a, c) ^{40}Ca + ^{40}Ca and (b, d) ^{197}Au + ^{197}Au with (closed symbols, left panels) and without (open symbols, right panels) the largest fragment. Lines are only to guide the eye.

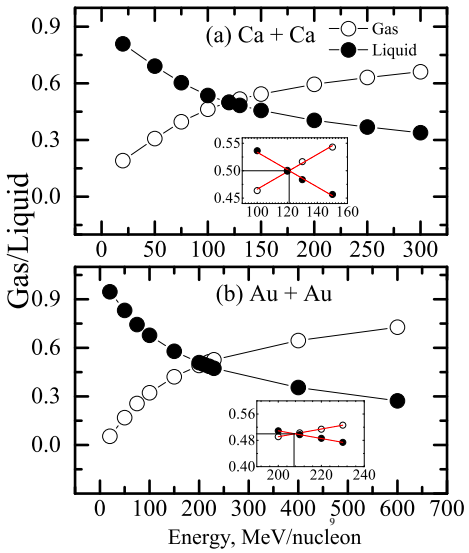

Figure 3. The energy dependence of the normalised yield of the gas and liquid content for the reactions of (a) ^{40}Ca + ^{40}Ca and (b) ^{197}Au + ^{197}Au without momentum dependent interactions. In the inset, the yield is shown at energies close to cross-over energy, with lines representing the linear fit. Lines are only to guide the eye.

Further, we have investigated the simultaneous behaviour of yields of free nucleons (gas/vapor phase) and bound nucleons (liquid phase) *vs.* beam energy. Note that in previous studies energy dependence of the gas-liquid has been defined in multiple number of ways [12–15]. Different studies have reported different definitions for a liquid and vapor phase. We have defined the gas phase to consist of fragments with $A_f = 1$ and all fragments with $A_f > 1$ to be the part of liquid phase. In Figures 3 we have shown the mass normalized yields of free nucleons (gas phase) and bound fragments (liquid phase) as a function of incident energy for the collisions of ^{40}Ca + ^{40}Ca and ^{197}Au + ^{197}Au without momentum dependent interactions. With increase in the incident energy, yield of free nucleons (gas phase) increases as at higher energies collisions become more violent, due to which system breaks into free particles. This leads to the increased gas content (open symbols) and decreased liquid content (closed symbols). The energy at which gas phase dominates the liquid phase, *i.e.* when yield of free nucleons becomes more than 50% of the total system mass, is considered as onset of vaporization. In the inset, the yield is shown at energies close to cross-over energy, with lines representing the linear fit. These energy values for the ^{40}Ca + ^{40}Ca and ^{197}Au + ^{197}Au are close to 120 and 210 MeV/nucleon without momentum dependent interactions. Figure 4 displays effect of momentum dependent interactions on the normalized yield of free nucleons and bound

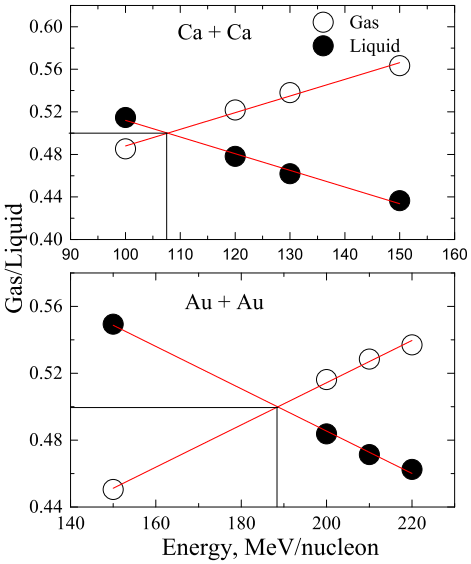

Figure 4. The normalized yield of free nucleons and bound fragments at energies close to cross-over energy for the collisions of (a) ^{40}Ca + ^{40}Ca and (b) ^{197}Au + ^{197}Au with momentum dependent interactions. The lines representing the linear fit. Lines are only to guide the eye.

fragments at energies close to cross-over energy with lines representing the linear fit. On introducing the momentum dependent interactions this energy is reduced significantly. This happens because of increased repulsions in the system, the number of binary nucleon nucleon collisions are reduced by 10–20%. Now the onset of vaporization occurs near 105 and 185 MeV/nucleon for the ^{40}Ca + ^{40}Ca and ^{197}Au + ^{197}Au, respectively. Therefore, we may say that momentum dependent interactions do play significant role in governing the onset of nuclear vaporization.

4 Conclusion

We have studied the system mass effects and influence of momentum dependent interactions on the energy of onset of vaporization using ^{40}Ca + ^{40}Ca and ^{197}Au + ^{197}Au system. It was concluded that average charge gives us crude value of energy of onset of vaporization and also do not show any significant influence of momentum dependent interactions. The gas/liquid content is successful in giving the absolute value of the energy of onset of vaporization. On introducing the momentum dependent interactions in the system, value of vaporization energy decreases.

References

[1] B. Jakobsson, et al., *Nucl. Phys. A* **509** (1990) 195.
[2] S.R. Souza, et al., *Nucl. Phys. A* **571** (1994) 159.
[3] Ch. Hartnack, et al., *Eur. Phys. J. A* **1** (1998) 151.
[4] J. Aichelin, *Phys. Rep.* **202** (1991) 233.
[5] R.K. Puri, J. Aichelin, *J. Comput. Phys.* **162** (2000) 245.
[6] N. Metropolis, et al., *J. Chem. Phys.* **21** (1953) 1087.
[7] P.J.M. Laarhoven, E.H.L. Aarts, *Simulated Annealing: Theory and Applications* (Reidel, Dordrecht, 1987).
[8] S. Kumar, R.K. Puri, *Phys. Rev. C* **60** (1999) 054607.
[9] C. Gale, et al., *Phys. Rev. C* **41** (1990) 1545.
[10] J. Singh, S. Kumar, R.K. Puri, *Phys. Rev. C* **63** (2001) 054603.
[11] J. Aichelin, et al., *Phys. Rev. Lett.* **58** (1987) 1926.
[12] J.Y. Liu, et al., *Phys. Rev. C* **70** (2004) 034610.
[13] J.Y. Liu, et al., *Chin. Phys. Lett.* **22** (2005) 65.
[14] B.A. Li, *Phys. Rev. Lett.* **85** (2000) 4221.
[15] W.M. Guo, et al., *Phys. Lett. B* **738** (2014) 397.